ISSN: 3067-8366
Research Article
Journal of Environmental Science, Sustainability, and Green Innovation

Estimating Point and Nonpoint Pollution within the Chippewa River Basin by Combining Chemical Mass Balance and Watershed Modeling

Sean Patrick Flynn*

M.S. University of Kansas, M.S Unity Environmental University, USA

***Corresponding author:** Sean Patrick Flynn, M.S. University of Kansas, M.S Unity Environmental University, USA.

Submitted: 16 May 2025 **Accepted:** 23 May 2025 **Published:** 29 May 2025

https://doi.org/10.63620/MKJESSGI.2025.1017

Citation: *Flynn, S. P. (2025). Estimating Point and Nonpoint Pollution within the Chippewa River Basin by Combining Chemical Mass Balance and Watershed Modeling. J Environ Sci & Sustain & Green Innov, 1(2), 01-13.*

Abstract

Urban rivers are increasingly facing pollution challenges due to the complex interplay of point and nonpoint sources, complicating effective water quality management. This study focuses on the Chippewa River Basin (CRB) in Minnesota, aiming to assess annual pollutant loading and identify hotspots for pollution. Utilizing a combination of Chemical Mass Balance (CMB) analysis and the PLOAD model, the research evaluates pollutant contributions from various sources. The CRB, characterized by a continental climate and significant agricultural land use, presents unique challenges in pollutant load estimation. Water quality sampling from multiple monitoring stations revealed that nonpoint source pollution, particularly from agricultural activities, significantly impacts water quality. The study highlights the effectiveness of integrating CMB and PLOAD for estimating nonpoint source loads, demonstrating that localized pollutant export coefficients yield more accurate results than generalized coefficients. Findings indicate that the upper segments of the CRB experience lower nonpoint source impacts compared to downstream areas, emphasizing the need for targeted pollution management strategies. This research contributes valuable insights for future water quality management efforts in various regions.

Keywords: PLOAD, Minnesota, Non-point Sources, Export Coefficients

Introduction

Urban rivers are becoming heavily polluted due to the extended release of pollutants from both point and nonpoint sources where the accurate pollution load to the river is difficult to determine based on the data quality and financial constraints which in turn makes water quality management more problematic [1]. Not only is the determination difficult to assess from the complexity of wastewater distribution from diverse sources but the lack of difference between urban point sources and no single pollution source [2, 3]. Pollutants from point sources including industries and institutions are becoming more of a threat to aquatic life based on poor allocation of waste and monitoring systems.

Furthermore, the monitoring of point sources within a given watershed can be difficult due to the limited time and costs [4]. While there are many problems in estimating pollutant loads within watersheds, there are different approaches and other pollution management practices that are considered the best. The common approaches for estimating pollutant loads are based on watersheds that need ample data [5-8]. The applications of the land use-based pollutant export coefficient approach and the mass balance approach fall into other pollutant load estimation strategies [9, 10]. Researchers recommend the study of input pollutant loads rather than the concentrations for effective water quality management [11].

Many researchers have used various techniques to estimate pollutant loads from diffused sources. One approach is to use the flux of pollutants based on the base flow separation method [12]. Another approach, while an indirect approach such as the

chemical mass balance (CMB) analysis is an economical and workable way for pollutant load estimation. The application of CMB was used by Raj et al. (2007), to determine the contribution of subsurface flow to a river in which, the load difference from the monitoring stations contributed to the flow from the subsurface source. This method was also used to estimate the internal processes within rivers, sediment, and the resuspension of chemicals, where the sediment plays the role of source/sink during both mass flux and CMB analysis [13, 14].

Furthermore, the approach was used for sideways pollutant load estimation in watersheds including India, North America, and Europe [15, 16, 13].

The goals of the research are to assess the annual pollutant loading from the contributions of both point and nonpoint sources to the Chippewa River Basin, to find hotspots for pollutant loading along with the calibration of export coefficients within the study area by combining CMB analysis and PLOAD.

Study Area

The Chippewa River Watershed is one of many major watersheds within the Minnesota River Basin. The river basin can be found in west central Minnesota and is about 2,084 square miles. The Chippewa River flows south towards the Minnesota River and the distance of the stream network is 2,091 miles. 1,567 miles of the stream network are considered intermittent and the other 525 miles are considered perennial streams (Minnesota River Basin Data Center, n.d.). The study area (Figure 1) is classified as a continental climate that has freezing winters and sweltering humid summers (St. Cloud State University, n.d.). The annual minimum temperature is 31 degrees Fahrenheit, and the annual maximum temperature is 55.4 degrees Fahrenheit with an annual rainfall of 2.14 inches (U.S. Climate Data, 2024). The bedrock of Minnesota is made of various rocks that include sandstone, shale, dolostone, and finally, limestone. Some of the rock layers are over 1,500 feet thick (University of Minnesota, 2000). The origins of toxins that are found in both surface and groundwater include mercury levels in soil, domestic sewage, and industrial wastewater that are washed into surface water or in groundwater via leeching. Other toxins that can be found occur through both hazardous waste sites and agricultural sites (Minnesota State University, 2004). Large-scale industries within the CRB release wastewater into the river before treatments happen, allowing the pollution load to increase, which makes water quality uncontrollable [17]. Roughly 75,000 years ago the Wisconsinan Episode left sediment from glaciers, outwash plains, till, lake plains, and moraines. Furthermore, the state also experienced several lobes that included Superior, Rainy, and Wadena lobes [18].

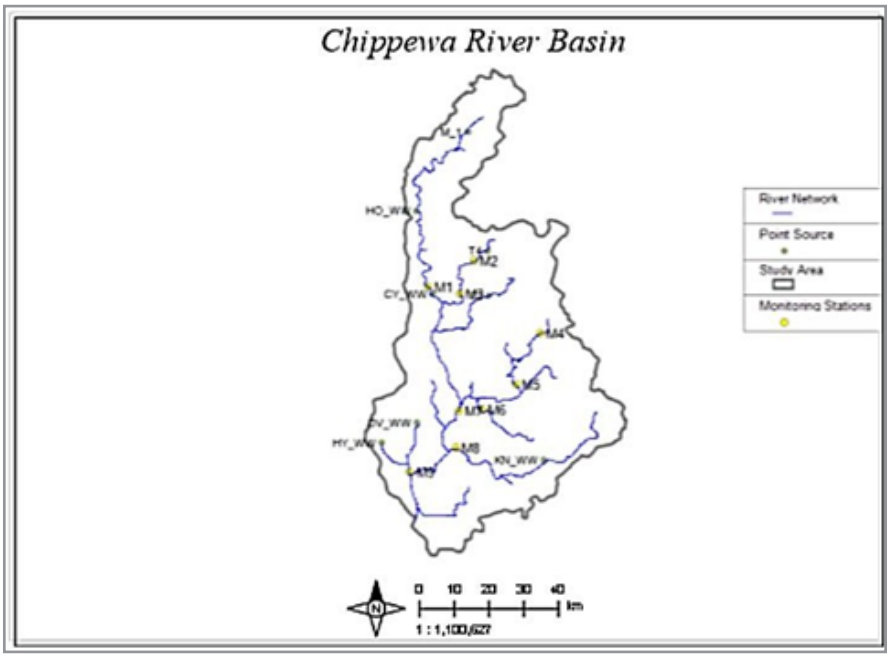

Figure 1: The Chippewa River Basin (CRB) water quality monitoring stations and point source locations.

Water Quality Sampling and Flow Simulation

For the pollutant load estimation in CRB water samples were collected from 9 main channel water monitoring stations (Table 1) and 9 tributaries and point sources (Figure 1 and Table 2). The instruments and analytical methods that were used for analysis are found within Table 3. All of the analytical techniques were done per examining both water and wastewater [19]. The gauge data for the Web-based Hydrograph Analysis Tool (WHAT) modeling calibration was collected from the USGS website (USGS, 2025). The WHAT model calibrated on the Little Chippewa River (LCR) outlet to simulate and create flow from the different monitoring stations, along with flow and concentration. The flow that was generated by WHAT for the monitoring stations was then drafted into the FLUX32 software for the estimation of pollutant loads.

Table 1: Main channel monitoring stations and locations in CRB.

Code	Station Name	Latitude	Longitude	Area (ha)
M1	Chippewa River near Cyrus	45.63163	-95.7381	400
M2	Little Chippewa River near Lowry	45.69996	-95.567	54
M3	Little Chippewa River near Starbuck	45.6144	-95.6203	96.2
M4	East Chippewa River near Terrace	45.50941	-95.3236	94.4
M5	Each Chippewa River near Swift Falls	45.37635	-95.4145	200
M6	Mud Creek near Benson	45.31274	-95.5417	85
M7	Chippewa River in Benson	45.31107	-95.6253	1270
M8	Shakopee Creek near Pennock	45.20996	-95.1892	352
M9	Cottonwood Creek near Big Bend City	45.15163	-95.8064	105

Table 2. Identified point sources near CRB, station locations, flow rates, and characteristics.

PS †	Latitude	Longitude	Q	Characteristics
M_1	46.02057	-95.5825	8410.267	Main Tributary Load
HO_WW	45.83056	-95.7833	7192.282	City of Hoffman Wastewater
T2	45.60833	-95.5167	545.0988	City of Starbuck Wastewater
T3	45.96667	-95.5833	340.687	City of Brandon Wastewater
HY_WW	45.25167	-95.9083	24605.18	City of Holloway Wastewater
DV_WW	45.28167	-95.7533	1892.706	City of Danvers Wastewater
T4	45.705	-95.5167	37854.12	Major pollutant load
CY_WW	45.61372	-95.7202	12946.11	City of Cyrus Wastewater
KN_WW	45.19167	-95.315	567.8118	City of Kerkhoven Wastewater

†Point source; Q is the mean flow rate (m3/d).

Table 3. Analytical techniques used for the analysis of selected constituents in CRB.

No	Parameter	Analytical Method	Equipment
1	BOD	Modified Winkler's Method	BOD Incubator
2	TDS	Gravimetric Method	Drying Oven, Desiccator
3	COD	Dichromate Method	COD Digester, Heating Block
4	PO4-P	Colorimetric	HACH DR-2800
5	NOx	Colorimetric	UV-VIS Spectrophotometer
6	TKN	Kjeldahl Method	Kjeldahl Flasks
7	TSS	Gravimetric Analysis	Glass-Fiber Membrane

CMB Analysis and Uncharacterized Nonpoint Source Load

Nonpoint source pollution is a source of pollution in water throughout the world and can be challenging based on the uneven distribution from various entry points [20-23]. Many software models have been developed to create an estimate for pollutant loads in rivers by using various mathematical equations to calculate estimated pollution source loads. FLUX32 was developed by the Minnesota Pollution Control Agency (MPCA) to create an estimated pollutant load that is carried by both streams and tributaries (Minnesota Pollution Control Agency, n.d.). The software requires datasets that include event-based pollution concentration and flow with gauge readings or output of river flow for a given period [24]. FLUX32 uses six different methods for calculating pollutant load and each method depends on the sampling approach and the variability of both flow and concentration [25].

Method six (regression applied to individual flows) was used for pollutant load calculation in CRB.

$$W_i = \sum exp\left[a + (b+1)\ln(Q_i) + \frac{SE^2}{2}\right] \quad (1)$$

where Qi = mean flow on day i (m3/s), ci = measured constituent concentration (mg/L), a = intercept of ln(c) vs. ln(q) regression, b = slope of ln(c) vs. ln(q) regression, S2 = standard error of estimate for ln(c) vs. ln(q) regression and q is instantaneous flow (m3/s), Wi = pollutant load/flux (kg/yr).

In CRB, point source loads were calculated by the product's average discharge rate of wastewater effluents and the mean concentration, in which a similar approach was used by (Jabbar & Grote, 2019), and the load from various tributaries was calculated using FLUX32. This is based on that point source loads are considered both stable and insignificant changes occur in the seasons [26, 27]. Also, calculations were done by using upstream-downstream CMB analysis combined with PLOAD, which is a watershed model.

The term uncharacterized nonpoint source load was used because the term includes unidentified point source and unrecognized nonpoint source loads, which used a similar description was used [28]. A simple mass balance approach by means of upstream-downstream can be used to estimate the initial pollutant load from a broader context [29].

$$\sum Q_D C_D - \sum Q_{UI} C_{UI} + \sum Losses = \sum L_i \quad (2)$$

where QD = river flow at the downstream station, CD = downstream constituent concentration, QUi = flow of a river at a river section upstream, CUi = upstream constituent concentration, Σ Losses = the sum of all losses in the stream, Li = is the net load.

The above approach was used in CRB lateral diffuse pollutant load estimation for two reasons. The first reason deals with the span length between the monitoring stations is small which indicates the loss is at a minimum and neglected. The second reason is the river components have the assumption of being mixed. With the simple mass balance equation (Equation (2)), the term ΣLi means that there are contributions from nonpoint source loads and not the net load at a given point, but combining all the loads, losses, and generations, which could be due to settlement, resuspension, and decay [30].

Watershed Model Selection

There have been many watershed models that have been developed along with various studies that determined pollutant loads from sources at the catchment scale that includes hydrological simulation program-FORTAN(HSPF), agricultural nonpoint pollution model (AGNPS), pollutant load (PLOAD), soil and water assessment tool (SWAT), and finally stormwater management model (SWMM) [31-35]. For the Chippewa River Basin, the PLOAD model was used for the study area and was integrated with the CMB analysis approach that was set up using water quality data [1]. PLOAD has the capacity and the adaptability to model different watersheds and is recommended for nonpoint source pollution management [36, 1].

PLOAD is a model plugin through BASINS (better assessment science integrating point and nonpoint sources) that estimates nonpoint source loads at the catchment level that is interpreted as annual loads (USEPA, 2001). The model combines point source and GIS-based land use data that estimates nonpoint source load contributions from the different land use categories by two different approaches. The approaches are export coefficient and the simple method.

$$L_p = \sum p \, (L_{PU} \times A_u) \quad (3)$$

where Lp = pollutant load (kg/yr), LPU = pollutant export coefficient for each land use (kg/ha/yr), AU = area by certain land use, ha.

Pollutant Export Coefficient

The export coefficient (ECf) is the amount of pollutant load transported over a given time [37]. Estimating catchment nonpoint source contribution by ECf, land use is automatically assumed to contribute to the pollutant load and is expressed by kg/ha/yr. The watershed shape file was delineated using ArcSWAT, where the land use within the study area is mainly dominated by agriculture and forested wetlands (Figure 2). Agriculture land use has the highest percent coverage at 79.2%, followed by forested wetlands at 8.2%, water at 4.6%, urban land at 4.3%, mixed forest at 2.7%, rangeland at 0.64%, and finally, bare land at < 0 %.

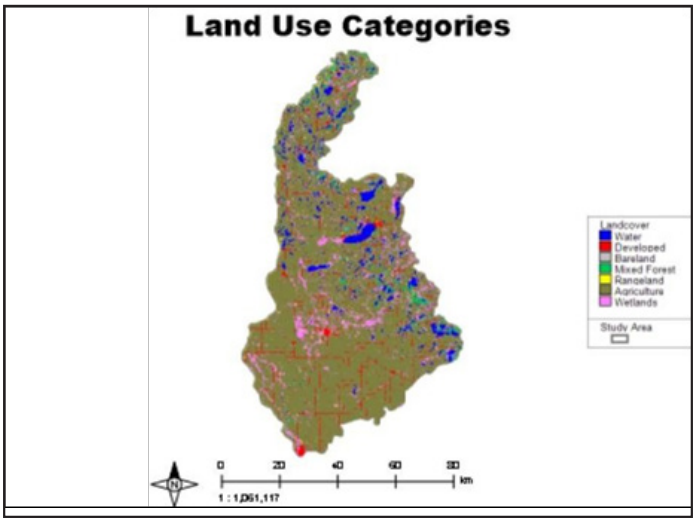

Figure 2: Land use map of the study area.

Pollutant load using export coefficients based on precipitation induced pollution can be expressed by;

$$L_{i,j} = \sum_{k=1}^{n} \left(E_{k,j} \times A_{k,j} + P_{i,j} \right) \quad (4)$$

where Li,j is calculated load of constituent i at the sub catchment outlet j (kg/yr); n is the number of land uses contributing; Ek,i is the export coefficient of land use k for the constituent i (kg/ha/yr); Ak,j is the area of land use k for the sub catchment j; Pi,j is precipitation-induced constituent i load at a sub catchment j (kg/yr). Pi,j is assumed negligible in basin.

For pollutant ECf in PLOAD, we reviewed literature values from Egypt, Japan, Lithuania, United States United States Envi-

ronmental Protection Agency, Ethiopia, China, Canada, Rwanda, Philippines, and Kenya [38-49, 33, 11]. Table 4 outlines the export coefficient for both nutrients and pollutants from case studies that were selected for estimation purposes in CRB.

Table 4: Export coefficient from case studies (kg/ha/yr) for pollution load (PLOAD) calibration in CRB.

Pollutants Export Coefficient from Case Studies in kg/ha/yr							
Land Use	BOD	COD	TDS	TN	TP	NO_x	PO_4
Water	50[m]	50[m]	10–150[l]	21.96–73.45[g]	1.99–6.55[g]	0.46[e]	10.11[i]
Developed	1833[e]	1952[e]	292[a]	20.87–35.73[m]	0.16–0.84[e]	91.44[b]	1.73[c]
Barren	3.29*	40[f]	100[l]	0.51–6[b]	0.12[e]	67.29[j]	4.81[i]
Mixed Forest	6.3[n]	12.3[n]	250[i]	6.24–10.36[m]	0.03–0.45[e]	2.12[e]	0.71[c]
Range Land	0.54[c]	0.52[c]	24–101[i]	3.2–14[b]	0.35–0.45[e]	0.46[c]	2*
Agriculture	68[e]	90[d]	45.6[e]	2.82–41.5[d]	0.126–1.348[e]	34.32[b]	36.34[i]
Wetlands	4.1[f]	29.4[f]	52[f]	1.1[f]	0.2[f]	0.4[f]	11.35[n]

Selection of Export Coefficients for PLOAD Calibration in CR in kg/ha/yr							
Land Use	BOD	COD	TDS	TN	TP	NO_x	PO_4
Water	50	50	150	73.45	6.55	0.4	40.91
Developed	1833	1952	292	35.7	0.84	91	1.73
Barren	3.29	40	100	6	0.12	67	19.46
Mixed Forest	6.3	12.3	250	10.36	0.45	2.12	0.71
Range Land	0.54	0.52	101	14	0.45	0.46	2
Agriculture	68	90	45.6	41.5	1.05	34.32	36.42
Wetlands	4.1	29.4	52	1.1	0.2	0.4	11.35

Estimated value from the PLOAD user guide (USEPA PLOAD, 2001); r* value based on grassland value.

Calibration and Validation of PLOAD

PLOAD uses data that is GIS based and includes land use, watershed boundaries, pollutant loading rate (ECf), rainfall, best management practices (BMPs) imperviousness, and finally point sources that is used for estimation purposes. Once the ECf is assigned for land use, PLOAD was then calibrated by using non-point source loads through CMB analysis and validated by using other data for optimization purposes through ECf and then finally measured through CMB. The PLOAD model was then further evaluated by comparing CMB analysis with the output of the model until the total error percentage between both measured and model- predicted values became either zero or as close to zero as possible. Excel solver was used because there is not a direct calibration possibility. The objective with Excel Solver is to refine the minimal amount of percentage with the error of becoming a zero value. The GRG nonlinear optimization was used based on localized optimum solution. The performance of the model was checked by;

$$\% ES = \frac{MLP - PPL}{MPL} \quad (5)$$

where ES is an error of estimation, MPL is measured pollutant load, PPL is PLOAD predicted load.

Results and Discussion

The study represents the pollutant load for the selected segments of both the CRB and the monitoring stations within the catchment outlets. It also measures the major hotspots for pollutants within the watershed and the pollutant contributions of different land uses.

Point Source Loading in CRB

The pollutant load from the point sources in CRB was much smaller than the tributaries based on the higher flow rate and the pollution level of tributaries than the point sources. But M7-M9 Figure 1 was heavily loaded from point source pollution which contributes significant pollution to CRB based on wastewater facilities. Furthermore, the polluted Chippewa River that joins the main river upstream from M1 and the tributary receives a lot of wastewaters that joins at the main river near M3, expanding the pollutant load in CRB. The load contribution from M7 was extremely high due to the vast amount of water consumption from the local wastewater facility that has a high flow rate. Table 5 explains the load that contributes from point sources to CRB. From the point source load summary in Table 5, the contributing stations HO_WW, T2, and KN_WW were incredibly significant for CRB organic and nutrient pollution.

Table 5: Summary of point source loads of selected physio-chemical constituents in CRB (t/yr).

Constituent Load in CRB (t/yr)								
Point Source	**MS†**	**BOD**	**COD**	**TDS**	**TN**	**TP**	**NO_x**	**PO_4-P**
M_1	M1	275.95	2523.82	1980.25	266.66	16.59	207.02	20.19
HO_WW	M1	646.64	6276.18	4448.41	644.57	40.2	500.11	49.59
T2	M7	813.69	7589.15	5540.08	750.1	46.92	582.14	57.52
HY_WW	M9	243.16	2431.35	1688.88	257.83	16.16	199.3	19.97
DV WW	M9	310.5	3096.67	2162.08	372.92	20.57	254.22	25.41
T4	M2	482.97	4643.62	3484.43	475.08	29.35	372.92	36.12
CY WW	M3	266.65	2636.86	1845.59	274.11	17.15	212.8	21.19
KN_WW	M8	653.53	6319.95	4640.03	659.32	40.72	507.84	49.93
M4	M5	466.96	4297.04	3230.92	449.54	27.75	346.99	33.94

MS† is downstream monitoring station where the point source load is contributing; T = tributary; WW = Wastewater Plant; HO, HY, DV, CY, KN = local cities; M = main channel.

MS† is downstream monitoring station where the point source load is contributing; T = tributary; WW = Wastewater Plant; HO, HY, DV, CY, KN = local cities; M = main channel.

Flow Simulation and Pollutant FLUX in CRB

The WHAT calibration at ECR was used to generate the flow within the CRB sub- catchment outlets in which the model output with instantaneous flow and pollutant concentration was used within the FLUX32 software for calculating pollutant loads. Furthermore, WHAT simulated the flow very well in both Figure 3 and Figure 4 with the R2 and NSE values of 0.86 and 0.77 while during calibration with values being 0.69 and 0.56. The indicators for model performance (R2 and NSE) fall into the acceptable ranges to interpret the model output. Figure 3 shows some deviation between both simulated and observational peaks which can possibly be due to the performance of the model. The hydrological performance of the model based on the Nash-Sutcliff (NSE) was found to be 0.77 and 0.86 during both calibration and validation within the study area falls within the range of good for interpretation, and the deviation between both observed and simulated flow is interpreted by error [50]. Comparable results were reported in other places with nearly similar trends between both model simulation and observations in the works [51-53].

While there was some deviation between the simulated and observed values at some of the peak points, the indicators for modeling performance (the Nash-Sutcliff) suggest that the model's output can be interpreted with acceptable accuracy. The WHAT-generated sub-catchment outlet flow was used for calculation purposes within FLUX32. The residual plot of bias (as the slope) for different variables within the catchment outlets within CRB was in the range of 0-0.07, which is very reasonable. The plot of slope significance fell in the range of 0.86-0.94. The coefficient of variation (CV) has a recommended range between 0 to 0.2 during flow-weighted load calculation and in CRB. The CV showed results within the range of 0.14-0.197, which is great. The pollutant load calculation in CRB using FLUX32, the outlier was checked by testing the significance level, $p \leq 0.05$.

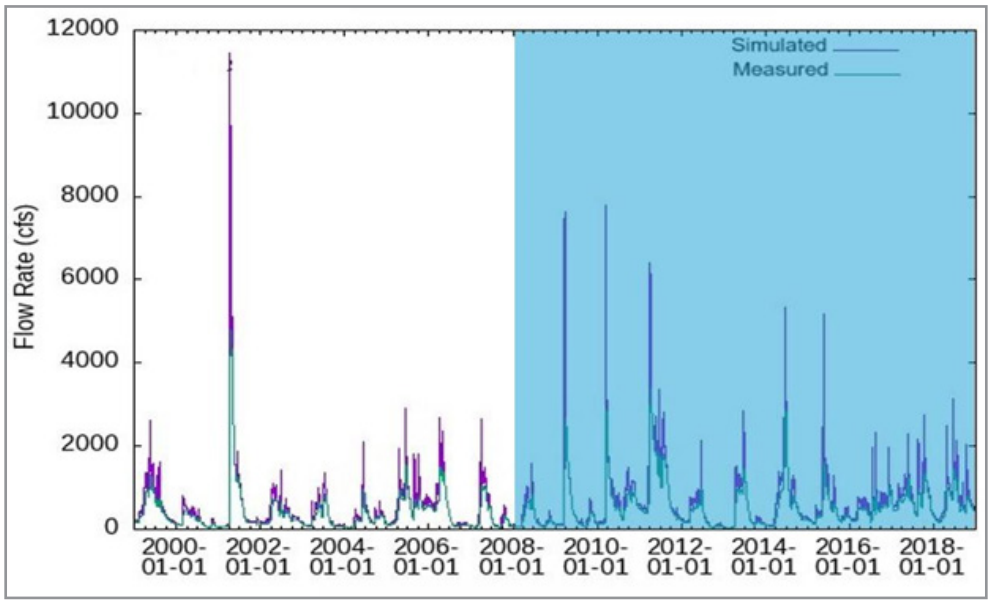

Figure 3: Web-based Hydrograph Analysis Tool (WHAT) simulation for flow at East Chippewa River (ECR) (calibration and validation). Validation is transparent turquoise.

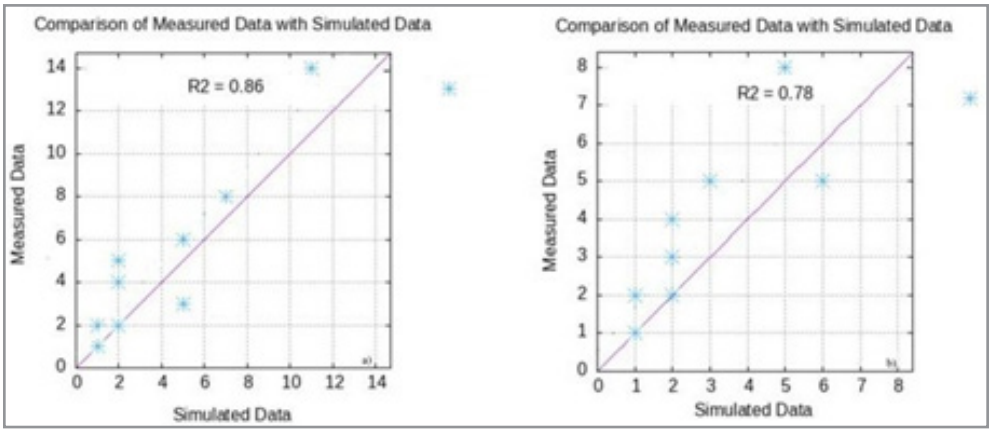

Figure 4: Plot of WHAT simulated versus observed flow in ECR (a) calibration and (b) validation (black diagonal line is a one to one (equality) line).

Chemical Mass Balance and Differential Load within CRB

After the loads were calculated at each of the sub-catchment outlets by FLUX-32, the CMB analysis was performed by using the upstream-downstream mass balance approach (Equation (2)) in order to determine the differential load. Similar approaches were also followed [54, 55, 28]. CMB analysis from each monitoring station (Table 6) shows that the prevalence of differential non-point source loads at the upstream segments of the CRB with the highest differential loads from calculations were BOD, COD, and TDS, which can be seen at segment outlets M7, M8, and M9. The influences of uncharacterized nonpoint sources show the highest significance (Figure 5). The areas were dominated by agriculture and wetland (small-intermediate) land uses. The contribution of organic pollution from nonpoint sources persisted within the study area where the differential BOD level was the maximum and was observed at M9 with 2592.87 t/yr where the station is downstream from two major wastewater plants. Furthermore, the maximum COD differential load from the non-point source was observed at the same station with the calculated load of 4014.59 t/yr and contributed to the sub-catchment that has an area of 13325.89 ha, that is followed by M8 and M7, with contributed the load of 3116.25 t and 2954.87 t. Also, high BOD depletion was observed at the downstream stations M8 (2188.5 t/yr) and M7 (2954.87 t/yr) where the impact of nonpoint sources is assumed to be nonsignificant. This shows the possibility of the river having high rates of recovery from self-purification processes [56].

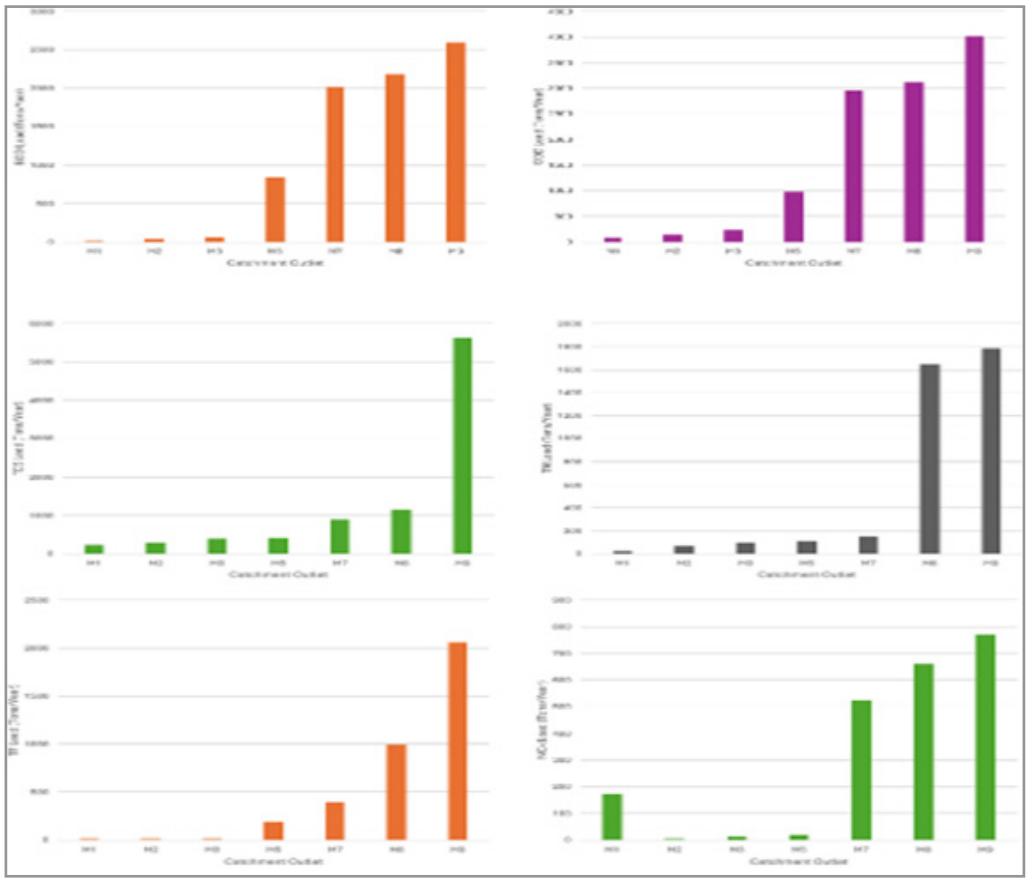

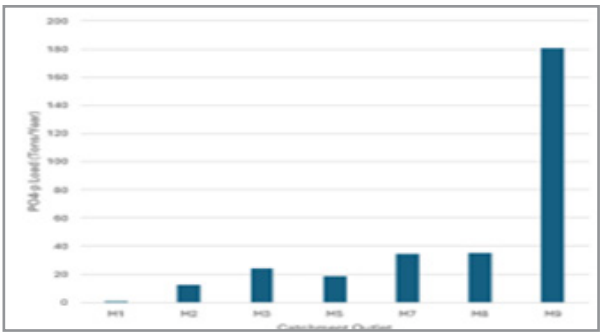

Figure 5: Nonpoint source pollutant loads at selected catchment outlets of CRB (t/yr).

Table 6: Differential nonpoint source pollutants load at CRB monitoring stations with chemical mass balance (CMB) analysis.

Catchment Outlet Differential Load (t/yr)							
Pa	M1	M2	M3	M5	M7	M8	M9
BOD	13.48	38.08	66.96	844.83	2015.45	2188.5	2592.47†
COD	79.96	143.57	230.17	978.9	2954.87	3116.25	4014.59
TDS	231.21	283.67	397.77	416.94	883.45	1162.9	5631.01
TN	24.63	69.01†	98.09†	111.08†	151.58	1650.91	1786.2
TP	0.59	4.53†	11.48†	191.79†	394.07†	999.82†	2063.8†
NO_x	174.96	1.54†	13.33	18.7†	521.47	662.34	770.76
PO_4-P	0.97†	12.51	23.85	18.35†	34.15	35.29	180.56

Pa = parameters; differential load = incremental load of the downstream station relative to the upstream station/s; † deficit (sink).

High PO4-P differential loads were calculated at the downstream stations that are characterized by small and medium agriculture persisting at M9 (180.56 ton/yr), followed by M8 (35.29 ton/yr), and finally M7 (34.15 ton/yr). The area is portrayed by agriculture and wastewater treatment plants. Furthermore, in (Table 6) the high differential load from TN was calculated at monitoring stations M7(151.58 t/yr), M8 (1650.91 t/yr), and M9 (1786.2 t/yr) while stations M2, M3, and M5 were identified as areas with TN sink. BOD, COD, TDS, and TN were the prevalent nonpoint pollution sources within the middle and downstream segments, which indicates the impact of washout from agricultural and wetland use [57]. The CMB analysis within CRB showed that most of the organic waste loading came from the middle segment, where the sink for the pollutants was found further downstream. The CMB analysis in CRB also showed that NOx, TP, and PO4-p had sinks at most of the catchment outlets. Stations M7-M9 are the recognized sink areas for nutrient and organic pollution that's located within the middle and downstream segments of CRB. A finding by Elósegui et al. (1995) showed the nutrient load within a river in Northern Spain was contained within the middle segment of the river [58]. The station M8 is the place where the organic pollutants are degraded, and the area was identified as a huge nutrient sink. It is a place that has federally protected areas, which may allow for the reduction of nonpoint source loading contributions. Compared to the downstream and middle catchment outlets, upstream segments have lowered nonpoint source contributions, in which a similar result from Hema & Muthalagi (2009) on the Hindon River in India. This may be based on the flow being low, less human influence, and buffer zones being present [59].

From the CMB analysis (Figure 6) most of the constituents within the upstream section of CRB (M1-M3) have the minimum differential load and show the reduction in the impact of nonpoint source pollution. The differential loads of TP, NOx, and PO4-P show most of the sinks can be observed within the middle and lower segments of CRB, where the river banks are protected by wetlands at M7 and M8 [60]. The maximum loading of nutrients that include TN, NOx, and PO4-P was recorded at M9, which is also the major sink for BOD. Interestingly, M8 was found within an area where TN and NOx have a positive differential load [61]. The station can be found downstream from the discharge point of a wastewater treatment plant and falls within small-scale agriculture [62].

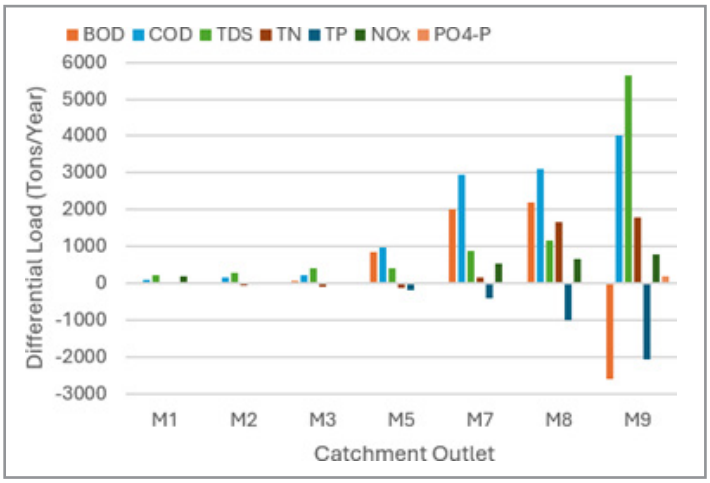

Figure 6: Differential pollutants load calculated at selected monitoring stations in CRB (t/yr).

Integration of CMB-PLOAD with Atypical Nonpoint Loading

The loads that were calculated at the selected CRB sub catchment outlets by CMB were used for the purposes of PLOAD calibration and the selected ECf for CRB was used for the initial estimation for calibration purposes. During the calibration of PLOAD within Excel Solver, the EFc were used as independent variables with the ranges being constraints by setting both the upper and the lower bounds of the ECf from literature to be used for optimization purposes. The total percentage of errors from the calibration and preoptimization stage for BOD, COD, NOX, PO4-P TDS, TN, and TP were 1469%, 3464.81%, 229%, 545%, 2036.46%, 350.62%, and finally, 260%. After optimizing the ECf within Solver, the average percentage of relative error dropped to 6.71%, 33%, 6.42%, 21.5%, 15.85%, 2.85%, and 7.85%. Furthermore, the sum of errors in COD was higher than BOD, which resulted with the total sum of error of 3464.81% at preoptimization, which was ascribed by the station number M9, at the point in which PLOAD underestimated both components at the station [63]. The PLOAD prediction for TDS was pretty accurate, with the total relative error with all the monitoring stations before optimizing found to be 2036.46% and sharply dropped to 15.85% after the optimization. The PLOAD model overestimated the TDS load within the upstream section of CRB (M1, and M7-M9), whereas the model underestimated the TP in CRB at the downstream segment of the river [64]. There were higher total errors that were recorded located at smaller catchments of CRB than in larger catchments. Zinabu et al. (44) came up with similar findings within the Kombolcha catchment in Ethiopia [65].

From the optimized ECf, agriculture, and wetland use ECf varies greatly based on the different subtypes of land use and shows a significant variation. The forest land-use category shows the minimum change with the loading of constituents across monitoring stations. This could be based on the area coverage within the watershed. PLOAD was then rerun using the median and mean values from both the optimized and calibrated ECf. While the median ECf gives the minimum total percent error to the mean value, hence, high variations in the ranges of the ECf made the loads vary greatly, the loads calculated by both the mean and median for the ECf, these values were deemed not acceptable [66].

The optimized ECf values show that the usage of both average and median values results in an underestimation of pollutant loads at different catchment outlets, while there are overestimated values on other catchments. This means that using area-specific ECf is more acceptable and is more effective with better pollutant value loads within CRB. The study that was conducted by Shrestha et al. (2008) recommends the use of area-specific and the development of localized ECf for effective calculations. The optimized values can also be interpreted well within CRB and used to manage nonpoint source pollution load within the catchment. The PLOAD was validated for another dataset without the change in the optimized export coefficient and the error calculated from the model was good enough for more interpretation. The percentage error between PLOAD predicted and measured values for BOD, COD, TDS, TN, and TP during validation was 16.42%, 6%, 9.7%, 16.7%, 8.6%, 11.52%, and 12.5%.

The calibrated pollutant ECfs showed that agriculture land use has varying export coefficients that are significant. The pollutant loading rate for agriculture land use ranged from 26.21-1062.77 kg/ha/yr, 217.9-1813.76 kg/ha/yr, and 512.61-2496.47 kg/ha/yr for BOD, COD, and TDS and varies within the different subtypes of agricultural land use (Cropland, Confined feeding ops, and other Agriculture land use) and location. Agriculture land use is dominated by cropland and pasture where other agricultural land uses have lesser rates [67]. The agricultural land use pollutant ECf for TP and TN greatly varies from 0.92-2332.93 kg/ha/yr and 14.85-897.71 kg/ha/yr. The high variation in ECf spatially is due to the high difference with the impact of nonpoint sources among different agricultural land uses. The upstream agricultural land use has less pollutant loading than both the middle and downstream catchments (Table 7).

The wetland use for all the pollutant loads was sensitive regarding the impact within CRB. The contribution of wetlands to the nonpoint COD load was constant within the range of 330.2kg/ha-2690.65 kg/ha/yr, and the acceptable volume of EFc for TDS within the range of 143.39-3974.62 kg/ha/yr suggests that wetland use varies with contributions to the TDS loading rate. Furthermore, BOD, TN, and TP have an annual loading rate of 74.92 kg/ha-946.43 kg/ha, 373.14 kg/ha-1001.83 kg/ha, and finally 12.8 kg/ha-62.81 kg/ha from wetland use.

Table 7: Uncharacterized nonpoint source load in CRB by integrating CMB and PLOAD, t/y.

R‡	BOD	COD	TDS	TN	TP	NO_x	PO_4-P
M1	1985.59	7301.15	4226.72	2149.75	515.3	22.18	11.21†
M2	800.46	2379.13	6006.36	721.11†	312.95†	14.13†	21.65
M3	454.49	2209.03	6964.16	148.75†	1001.62†	35.22	34.08
M5	581.07	1240.22	3233.41	302.05†	1005.8†	408.6†	48.53†
M7	1673.57	6943.37	2388.42	1375.77	32.26†	51.8	12.5
M8	458.3	1111.67	747.42	339.08	204.62†	1203.43	70.43
M9	1528.97†	4900.1	5766.25	3142.5	3537.35†	1874.01	1536.88

†The loads in which the deficit was calculated using CMB analysis, but PLOAD estimated the value from sub catchments ECf; ‡ catchment outlets where PLOAD was calibrated and represents nonpoint source contributions.

Conclusion

The following major conclusions were drawn from the research findings. The application of both the chemical mass balance and PLOAD was used to estimate the nonpoint source load within the Chippewa River Basin, Minnesota, and was found to be effective. The approach shows there is more efficiency within the study area, which focused on both organic pollutants and the loading of nutrients based on the water quality data from monitored stations in the rivers. The major conclusions from this study are:

- Nonpoint source impacts within the upper stream segment of the CRB catchment was lesser than the downstream and middle segments based on the impact reduction of point sources that are not recognized, little areas of urban settlements, and land use management. Furthermore, the lesser rate of flow within the upper segments of the river may play a crucial role in the lowering of diffused load sourcing within the area.
- Combining CMB and catchment nonpoint source pollution models that include PLOAD can be both an effective and alternative approach for those areas that have problems with data scarcity.
- The nonpoint source pollutant load was high in areas where agricultural land is found, followed by wetland and open water which indicates where nonpoint source pollution management areas need to have a focus on.
- Local pollutant export coefficients were found effective and accurate for the approach of load estimation than using both the mean and median export coefficients. Although CMB has a higher accuracy for estimating differential nonpoint source load estimating, combining a non-complex watershed model is a better alternative with regards for a more accurate indication of diffused loads.
- There was some over and underestimation with PLOAD and some of the catchment outlets and when PLOAD was combined with CMB, the analysis showed results that were promising. The adaptation of the global export coefficient to localized conditions limits the integral modeling approach.
- Both pollutant and nutrient export coefficients that were developed within CRB catchment can be transferred to other catchments in other areas for similar applications for nonpoint source pollutant loading management. Both the effectiveness and accuracy of CMB for loading depends on frequency of collecting data, monitoring station distance, and finally finding and identifying the major point sources of pollution in relation to the river.

Integrating chemical mass balance and PLOAD can be a more viable option to estimate nonpoint source pollution levels in areas that have a lot of data or minimal data for water quality. In the future, studies can incorporate extensive long-term monitoring at larger catchments can be quite helpful for pollutant load management in rivers.

References

1. Delkash, M., Al-Faraj, F. A. M., & Scholz, M. (2014). Comparing the export coefficient approach with the Soil and Water Assessment Tool to predict phosphorous pollution: The Kan Watershed case study. Water, Air, & Soil Pollution, 225, 2122. https://doi.org/10.1007/s11270-014-2122-5
2. Gurung, D. P., Githinji, L. J., & Ankumah, R. O. (2013). Assessing the nitrogen and phosphorus loading in the Alabama (USA) River Basin using PLOAD model. Air, Soil and Water Research, 6, 23–36. https://doi.org/10.4137/ASWR.S11710
3. Ongley, E. D., Xiaolan, Z., & Tao, Y. (2018). Current status of agricultural and rural non-point source pollution assessment in China. Environmental Pollution, 158, 1159–1168. https://doi.org/10.1016/j.envpol.2008.09.047
4. Chen, D., Dahlgren, R. A., & Lu, J. (2013). A modified load apportionment model for identifying point and diffuse source nutrient inputs to rivers from stream monitoring data. Journal of Hydrology, 501, 25–34. https://doi.org/10.1016/j.jhydrol.2013.07.019
5. Hao, G., Li, J., Li, S., Li, K., Zhang, Z., & Li, H. (2020). Quantitative assessment of non-point source pollution load of PN/PP based on RUSLE model: A case study in Beiluo River Basin in China. Environmental Science and Pollution Research, 27, 33975–33989. https://doi.org/10.1007/s11356-020-09450-0
6. Huiliang, W., Zening, W., Caihong, H., & Xinzhong, D. (2015). Water and nonpoint source pollution estimation in the watershed with limited data availability based on hydrological simulation and regression model. Environmental Science and Pollution Research. https://doi.org/10.1007/s11356-014-4005-5
7. Liu, Y., Li, H., Cui, G., & Cao, Y. (2020). Water quality attribution and simulation of non-point source pollution load flux in the Hulan River basin. Scientific Reports, 10, 1–15. https://doi.org/10.1038/s41598-020-77661-z

8. Wu, L., Liu, X., & Ma, X. (2016). Spatio-temporal variation of erosion-type non-point source pollution in a small watershed of hilly and gully region, Chinese Loess Plateau. Environmental Science and Pollution Research, 23, 10957–10967. https://doi.org/10.1007/s11356-016-6321-9
9. Wu, L., Gao, J., Ma, X., & Li, D. (2015). Application of modified export coefficient method on the load estimation of non-point source nitrogen and phosphorus pollution of soil and water loss in semiarid regions. Environmental Science and Pollution Research, 22, 10647–10660. https://doi.org/10.1007/s11356-015-4252-1
10. Chen, Y., Zang, L., Shen, G., Liu, M., Du, W., Fei, J., & Yang, L. (2019). Resolution of the ongoing challenge of estimating nonpoint source neonicotinoid pollution in the Yangtze River Basin using a modified mass balance approach. Environmental Science & Technology, 53, 2539–2548. https://doi.org/10.1021/acs.est.8b06417
11. Shrestha, S., Kazama, F., Newham, L. T. H., Babel, M. S., Clemente, R. S., Ishidaira, H., Nishida, K., & Sakamoto, Y. (2008). Catchment scale modelling of point source and non-point source pollution loads using pollutant export coefficients determined from long-term in-stream monitoring data. Journal of Hydro-environment Research, 2, 134–147. https://doi.org/10.1016/j.jher.2008.09.001
12. Waseem, M., Koegst, T., & Tränckner, J. (2018). Groundwater contribution to surface water contamination in a North German low land catchment with intensive agricultural land use. Journal of Water Resource and Protection, 10, 231–250. https://doi.org/10.4236/jwarp.2018.103014
13. Berndtsson, R. (1990). Transport and sedimentation of pollutants in a river reach: A chemical mass balance approach. Water Resources Research, 26, 1549–1558. https://doi.org/10.1029/WR026i007p01549
14. Morris, A. W., Allen, J. I., Howland, R. J. M., & Wood, R. G. (1995). The estuary plume zone: Source or sink for land-derived nutrient discharges? Estuarine, Coastal and Shelf Science, 40, 387–402. https://doi.org/10.1006/ecss.1995.0039
15. Jain, C. K., Bhatia, K. K. S., & Seth, S. M. (1998). Assessment of point and non-point sources of pollution using a chemical mass balance approach. Hydrological Sciences Journal, 43, 379–390. https://doi.org/10.1080/02626669809492133
16. Dengler, E. L. (2017, May). Glacial geology. College of Science and Engineering, University of Minnesota. https://cse.umn.edu/mgs/glacial-geology
17. Dolan, D. M., & El-Sharawi, A. H. (1989). Inferences about point source loadings from upstream/downstream river monitoring data. Environmental Monitoring and Assessment, 12(3), 343–357.
18. Drewry, J., Newham, L., Greene, R., Jakeman, A., & Croke, B. (2020). An approach to assess and manage nutrient loads in two coastal catchments of the Eurobodalla region, NSW, Australia.
19. Hou, A., DeLaune, R. D., Tan, M., Reams, M., & Laws, E. (2009). Toxic elements in aquatic sediments: Distinguishing natural variability from anthropogenic effects. Water, Air, and Soil Pollution, 203(1), 179–191. https://doi.org/10.1007/s11270-009-0002-3
20. Lipps, W. C., Braun-Howland, E. B., & Baxter, T. E. (2023). Standard methods for the examination of water and wastewater (2022 ed.). American Public Health Association. https://www.standardmethods.org/
21. Morelli, B., Hawkins, T. R., Niblick, B., Henderson, A. D., Golden, H. E., Compton, J. E., Cooter, E. J., & Bare, J. C. (2018). Critical review of eutrophication models for life cycle assessment. Environmental Science & Technology, 52(17), 9562–9578. https://doi.org/10.1021/acs.est.8b00967
22. Park, Y. S., & Engel, B. A. (2014). Use of pollutant load regression models with various sampling frequencies for annual load estimation. Water, 6(6), 1685–1697.
23. Sekhar, C., & Umamahesh, N. V. (2004). Mass balance approach for assessment of pollution load in the Krishna River. Journal of Environmental Science & Engineering, 46(2), 159–171. PMID: 16649607
24. Vignesh, S., Muthukumar, K., Gokul, M. S., & James, R. A. (2013). Microbial pollution indicators in the Cauvery River, southern India. In On a Sustainable Future of the Earth's Natural Resources (pp. 363–376).
25. Yuan, L., Sinshaw, T., & Forshay, K. J. (2020). Review of watershed-scale water quality and nonpoint source pollution models. Geosciences, 10(1), 25.
26. Zhang, J., & Zhang, J. (2020). Discussion on non-point source pollution and control in water source areas. In Study of Ecological Engineering of Human Settlements (pp. 197–221).
27. Chen, J., Shi, W., & Jin, X. (2022). Pollutant flux estimation of the Lijiang River based on an improved prediction-correction method. Frontiers in Environmental Science, 10, 868404.
28. Hema, S., & Muthalagi, S. (2009). Mass balance approach for assessment of pollution load in the Tamiraparani River. International Journal of ChemTech Research, 1(2), 385–389.
29. Kuma, H. G., Feyessa, F. F., & Demissie, T. A. (2022). Impacts of land-use/land-cover changes on nutrient losses in agricultural catchment, southern Ethiopia. Water Supply, 22(5), 5509–5523. https://doi.org/10.2166/ws.2022.130
30. Alam, M. J., & Dutta, D. (2022). Application of a mathematical model for nutrient pollution assessment in a small catchment of the Latrobe River Basin, Australia. In Environmental Hydraulics. Volume 1 (pp. 413–418). CRC Press.
31. Li, Z., Luo, C., Jiang, K., Wan, R., & Li, H. (2017). Comprehensive performance evaluation for hydrological and nutrients simulation using the Hydrological Simulation Program—Fortran in a mesoscale monsoon watershed, China. International Journal of Environmental Research and Public Health, 14(12), 1599.
32. Wang, X., Yang, H., Cai, Y., Yu, C., & Yue, W. (2016). Identification of optimal strategies for agricultural nonpoint source management in Ulansuhai Nur watershed of Inner Mongolia, China. Stochastic Environmental Research and Risk Assessment, 30(1), 137–153.
33. Kipyego, S., & Ouma, Y. (2018). Analysis of nonpoint source pollution loading on water quality in an urban-rural river catchment using GIS-PLOAD model: Case study of Sosiani River. Civil and Environmental Research, 10(6), 70–84.
34. Santhi, C., Arnold, J. G., Williams, J. R., Dugas, W. A., Srinivasan, R., & Hauck, L. M. (2001). Validation of the SWAT model on a large river basin with point and nonpoint sources. Journal of the American Water Resources Association, 37(5), 1169–1188.

35. Lai, Y. C., Yang, C. P., Hsieh, C. Y., Wu, C. Y., & Kao, C. M. (2011). Evaluation of non-point source pollution and river water quality using a multimedia two-model system. Journal of Hydrology, 409(3–4), 583–595.
36. Xie, W., Li, J., Liu, Y., Peng, K., & Zhang, K. (2023). Evaluation of ecological buffer zone based on landscape pattern for non-point source pollution control: A case study in Hanjiang River basin, China. Journal of Hydrology, 626, 130341. https://doi.org/10.1016/j.jhydrol.2023.130341
37. Ma, X., Li, Y., Zhang, M., Zheng, F., & Du, S. (2011). Assessment and analysis of non-point source nitrogen and phosphorus loads in the Three Gorges Reservoir Area of Hubei Province, China. Science of the Total Environment, 412–413, 154–161.
38. Fleifle, A., Saavedra, O., Yoshimura, C., Elzeir, M., & Tawfik, A. (2014). Optimization of integrated water quality management for agricultural efficiency and environmental conservation. Environmental Science and Pollution Research, 21(13), 8095–8111.
39. Povilaitis, A. (2010). Source apportionment and retention of nutrients and organic matter in the Merkys River Basin in southern Lithuania. Journal of Environmental Engineering and Landscape Management, 16(4), 195–204.
40. Haith, D. A., Mandel, R., & Wu, R. S. (1992). GWLF: Generalized Watershed Loading Functions Version 2.0 user's manual. Department of Agricultural and Biological Engineering, Cornell University.
41. Brezonik, P. L., & Stadelmann, T. H. (2001). Analysis and predictive models of stormwater runoff volumes, loads, and pollutant concentrations from watersheds in the Twin Cities Metropolitan Area, Minnesota, USA. Water Resources Research, 37(1), 1–12.
42. Lin, J. P. (2004). Review of published export coefficient and event mean concentration (EMC) data (WRAP Technical Notes Collection, ERDC TN-WRAP-04-3). U.S. Army Engineer Research and Development Center.
43. Anderson, K. J., Adhikari, B., Schloegel, O. F., Mendonca, R. M., Back, M. P., Brocato, N., Cianci-Gaskill, J. A., McMurray, S. E., Bahlai, C., Costello, D. M., & Kinsman-Costello, L. (2024). We know less about phosphorus retention in constructed wetlands than we think we do: A quantitative literature synthesis. Ecological Indicators, 169, 112969. https://doi.org/10.1016/j.ecolind.2024.112969
44. Zinabu, E., van der Kwast, J., Kelderman, P., & Irvine, K. (2017). Estimating total nitrogen and phosphorus losses in a data-poor Ethiopian catchment. Journal of Environmental Quality, 46(6), 1519–1527.
45. Lu, J., Gong, D., Shen, Y., Liu, M., & Chen, D. (2013). An inversed Bayesian modeling approach for estimating nitrogen export coefficients and uncertainty assessment in an agricultural watershed in eastern China. Agricultural Water Management, 116, 79–88. https://doi.org/10.1016/j.agwat.2012.10.020
46. Jeje, Y. (2016). Export coefficients for total phosphorus, total nitrogen and total suspended solids in the southern Alberta region: A review of literature (pp. 1–22). Alberta Environment.
47. Wali, U. G., Nhapi, I., Ngombwa, A., Banadda, N., Nsengimana, H., Kimwaga, R. J., & Nansubuga, I. (2011). Modelling of nonpoint source pollution in Akagera Transboundary River in Rwanda. Open Environmental Engineering Journal, 4, 124–132.
48. Amaya, F. L., Gonzales, T. A., Hernandez, E. C., Luzano, E. V., & Mercado, N. P. (2012). Estimating point and nonpoint sources of pollution in Biñan River Basin, the Philippines. In Proceedings of the International Conference on Environmental Science and Development (ICESD) (Vol. 1, pp. 233–238). Hong Kong, China.
49. Moriasi, D. N., Arnold, J. G., Van Liew, M. W., Bingner, R. L., Harmel, R. D., & Veith, T. L. (2007). Modeling evaluation guidelines for systematic quantification of accuracy in watershed simulations. American Society of Agricultural and Biological Engineers, 50(3), 885–900.
50. Abbaspour, K. C., Rouholahnejad, E., Vaghefi, S., Srinivasan, R., Yang, H., & Kløve, B. (2015). A continental-scale hydrology and water quality model for Europe: Calibration and uncertainty of a high-resolution large-scale SWAT model. Journal of Hydrology, 524, 733–752.
51. Rostamian, R., Jaleh, A., Afyuni, M., Mousavi, S. F., Heidarpour, M., Jalalian, A., & Abbaspour, K. C. (2008). Application of a SWAT model for estimating runoff and sediment in two mountainous basins in central Iran. Hydrological Sciences Journal, 53(5), 977–988.
52. Shawul, A. A., Chakma, S., & Melesse, A. M. (2019). The response of water balance components to land cover change based on hydrologic modeling and partial least squares regression (PLSR) analysis in the Upper Awash Basin. Journal of Hydrology: Regional Studies, 26, 100640.
53. Jain, C. K., Singhal, D. C., & Sharma, M. K. (2007). Estimating nutrient loadings using chemical mass balance approach. Environmental Monitoring and Assessment, 134(1), 385–396.
54. Jain, C. K. (2000). Application of chemical mass balance approach to determine nutrient loading. Hydrological Sciences Journal, 45(4), 577–588.
55. Setiawan, A. D., Widyastuti, M., & Hadi, M. P. (2018). Water quality modeling for pollutant carrying capacity assessment using Qual2Kw in Bedog River. Indonesian Journal of Geography, 50(1), 49–56.
56. Elósegui, A., Arana, X., Basaguren, A., & Pozo, J. (1995). Self-purification processes along a medium-sized stream. Environmental Management, 19(6), 931–939.
57. Jabbar, F. K., & Grote, K. (2019). Statistical assessment of nonpoint source pollution in agricultural watersheds in the Lower Grand River watershed, MO, USA. Environmental Science and Pollution Research, 26(2), 1487–1506.
58. Minnesota Pollution Control Agency. (n.d.). Water monitoring resources. https://www.pca.state.mn.us/business-with-us/water-monitoring-resources
59. Minnesota River Basin Data Center. (n.d.). Chippewa Major Watershed general description. https://mrbdc.mnsu.edu/major/chippewa/descgen26.html
60. Minnesota State University. (2004, September 15). Toxics in the Minnesota River Basin. https://mrbdc.mnsu.edu/toxics-minnesota-river-basin

61. Raj, P., Lee, S., Lee, Y., Kanel, S. R., & Pelletier, G. J. (2007). Application of automated QUAL2Kw for water quality modeling and management in the Bagmati River, Nepal. Ecological Modelling, 202(3–4), 503–517.
62. Sekhar, M. C., & Sreenivasulu, D. (2003). Modelling nutrients contributed by overland flow from the Krishna River Basin. In Proceedings of the Diffuse Pollution Conference: Water Resources Management (pp. 20–23). Dublin, Ireland.
63. 41. Brezonik, P. L., & Stadelmann, T. H. (2001). Analysis and predictive models of stormwater runoff volumes, loads, and pollutant concentrations from watersheds in the Twin Cities Metropolitan Area, Minnesota, USA. Water Resources Research, 37(1), 1–12.
64. St. Cloud State University. (n.d.). Climate in Minnesota for international students. https://www.stcloudstate.edu/internationaladmissions/accepted-next-steps/climate.aspx#:~:text=The%20weather%20and%20climate%20of,temperatures%20begin%20to%20warm%20up.
65. U.S. Climate Data. (2024). Weather averages Glenwood, Minnesota. Temperature - Precipitation Sunshine - Snowfall. https://www.usclimatedata.com/climate/glenwood/minnesota/united-states/usmn0296
66. University of Minnesota. (2000). Minnesota at a Glance. Ancient tropical seas—Paleozoic history of Southeastern Minnesota. https://cdn.serc.carleton.edu/files/nagt/programs/teachingmaterials/paleozoic_bdrk.pdf
67. USEPA PLOAD: An ArcView GIS Tool to Calculate Nonpoint Sources of Pollution in Watershed and Stormwater Projects- version 3.0; United States Environmental Protection